

Investigating the Origins of Life: The Role of UV Light in Prebiotic Chemistry

Azra Haseki

under the direction of

Dr. Sukrit Ranjan
Massachusetts Institute of Technology
Earth, Atmospheric and Planetary Sciences Department

Research Science Institute
July 30, 2019

Abstract

In this study, we investigate the UV transmission in the oceans of the prebiotic Earth. We use previous experimental data to construct absorbtivity models for the prebiotic ocean, modern abiotic ocean, and a prebiotic lake. In doing so we take into account the distinct ion makeup of prebiotic and modern seawater. We investigate whether the absorbance of certain ions in the prebiotic ocean is additive, and come to the conclusion that for compounds of ferrous iron absorbance cannot be treated as additive. We find that appreciable energy could have only been delivered to the first 10 m of the prebiotic ocean. We also place constraints on the UV absorbance of prebiotic lakes, which contradict earlier research and impact origin of life pathway theories.

Summary

The question of how life first began on Earth has been investigated for centuries. In order to characterise the processes that affected the emergence of life on Earth, it is important to comprehend the conditions on prebiotic Earth, and ultraviolet (UV) light is of particular significance. In this study we investigate the UV transmission in the oceans of the prebiotic Earth. We construct models for the transmission of UV light for the prebiotic ocean, modern abiotic ocean, and a prebiotic lake using previous experimental data and compare them to clear modern ocean waters. Our UV transmission models place contraints on the environment in which life may have emerged.

1 Introduction

The question of how life first began on Earth has been investigated for centuries. In order to characterise the processes that affected the emergence of life on Earth, it is important to comprehend the conditions on prebiotic Earth. Understanding the conditions present on early Earth is central to assessing the viability of pathways theorised to have led to the formation of life.

Ultraviolet (UV) light is an important factor in characterising the conditions of prebiotic Earth. Due to its high energy, UV light (200-400 nm) has the ability to facilitate chemical reactions through photochemistry. UV irradiation can supply the energy necessary to excite electrons, ionise atoms, and break molecular bonds [1]. The ionisation of atoms results in free electrons, which can act as oxidising agents in further reactions. These changes allow molecules to engage in reactions that would not be possible in their ground states, powering possible origin of life pathways. It is also hypothesised that UV light may have served as a selector for the biological molecules that form the basis of life today. This mechanism functions through the photodegradation of complex hydrocarbons that are formed in idealised prebiotic Earth experiments yet are not instrumental in the formation of life. The relative UV resistance of the nucleobases that are the basis of current life point to UV light as a factor in the selection of biotic molecules.

For instance, the pathway proposed by Powner et al. points to the amplification of ribocytidine and ribouridine under UV light, ribocytidine and ribouridine being two of the nucleobases fundamental to the formation of life [2]. UV light also improves the RNA world model, which is a dominant origin of life theory [3, 4]. The ability to both replicate itself and encode for genetic information makes RNA a primary candidate to have made the transition from prebiotic chemical reactions to living organisms. However, in the absence of UV light two problems present themselves. Firstly, RNA molecules do not polymerise indepen-

dently and therefore cannot replicate and sustain life. The second is a high concentration of hydrocarbons not significant biotic processes being formed, which results in a significantly less chance of biotic molecules reacting with each other. Hence UV light's ability to both select biologically relevant molecules and power otherwise unfavourable reactions makes it a determining factor in prebiotic Earth models.

Previous work done on the UV environment on prebiotic Earth has identified that UV light may have been the most readily available source of energy for prebiotic chemistry. Examination of sulfide from a variety of Precambrian (4.6 billion - 541 million years ago) era rock samples reveals that before 2450 million years ago, sulfur fractionation occurred independent of mass [5]. This demonstrates that a strong energy source with enough energy to power the reaction for all isotopes, regardless of weight, was present. UV irradiation is thus known to be abundant in the prebiotic era, as atmospheric photochemical reactions are the only fractionation mechanism consistent with mass independent sulfur fractionation [6]. In addition, the prebiotic Earth lacked an ozone (O_3) layer and significant oxygen (O_2) in the atmosphere prior to the Great Oxygenation Event 2.3 billion years ago. Both O_3 and O_2 are substantial in shielding UV light, yet Pavlov and Kasting have identified that the atmospheric O_2 concentration must have been less than 10^{-5} of the present atmospheric level before 2.3 billion years. Had the oxygen concentration been higher, it would have reacted readily with the sulfur, removing all traces of mass independent fractionation [6]. Moreover, the early Sun emitted a higher fraction of its emission in the UV band [2]. The presence of mass independent sulfur fractionation, absence of significant concentrations of atmospheric oxygen, and greater fractional output by the early Sun thus characterise the prevalence and importance of UV light on prebiotic Earth.

In this study, we investigate the UV transmission in the oceans of the prebiotic Earth. We compare the UV transmission of our modeled prebiotic ocean with the UV transmissions of the clearest natural waters as measured by Smith and Baker, and our constructed abiotic

seawater [7]. In doing so we take into account the distinct ion makeup of prebiotic and modern seawater. We investigate whether the absorbance of these ions is additive, and come to the conclusion that for compounds of ferrous iron absorbance cannot be treated as additive. We also hypothesise that prebiotic seawater was less UV transmittant than modern abiotic seawater, and in the most part clearest natural waters.

2 Methods

In order to characterise the UV environment in the waters of the prebiotic Earth, we analysed and modeled the transmittance of pure water and different aqueous solutions. As is well known, when light travels through a medium, it interacts with the particles in the medium and is partially scattered and absorbed. For the purposes of this study, scattering is negligible and therefore we consider only absorbance. The emergent light at any depth is expressed by Beer-Lambert's Law:

$$I = I_0 \xi bc \quad (1)$$

where I is the intensity of emergent light at the given pathlength, I_0 is the incident light intensity, b is the path length in cm, c is the concentration of the solution in M (mol L^{-1}), and ξ is the molar absorptivity constant ($\text{M}^{-1}\text{cm}^{-1}$), which depends on the specific medium or solute.

In the case of a pure medium, such as water, the absorptivity coefficient is directly given in cm^{-1} , as there is no molar concentration. *Absorptivity* is given by bc . *Absorbance*, A , given by ξbc , is related to the transmittance of a solution through

$$T = 10^{-A}. \quad (2)$$

Transmittance is an expression of the ratio of light intensity that reaches the specified path length over the incident light intensity.

The lowest bound for UV light absorbance in aqueous solutions is given by pure water. In

order to obtain a lowest bound for the UV absorbance both in prebiotic and modern waters, we modeled absorbtivity coefficient values for pure water from 196 to 320 nm, taken from Quickenden and Irvin (1980) to find the transmittance for pure water at 1 cm, 1 m, and 10 m [3].

In order to compare the UV absorbance of prebiotic seawater with modern seawater, we then modeled the absorption and transmittance of the "clearest" modern ocean waters. We obtained values for the absorptivity coefficient [$K \lambda$] of these natural waters from Smith and Baker [7]. Smith and Baker characterised the "clearest" natural waters by their minimal organic material content. The measured values of these ocean waters served as a check for our modern abiotic ocean model as well as a basis of comparison for our constructed prebiotic ocean.

To model modern abiotic seawater and prebiotic seawater, we first obtained the ion makeup of both modern and prebiotic oceans. The two major components of optical significance of modern ocean water were found to be organic matter and tertiary matter. In order to compare modern and prebiotic seawater, modern abiotic seawater was modeled, as prebiotic ocean water would by definition not contain life elements. It is possible for prebiotic seawater to have contained organic molecules, however, and we included such organic molecules in our study seperately. The dominant ions for modern seawater were cited to be bromide (Br^-) at wavelengths shorter than 230 nm and nitrate (NO_3^-) for wavelengths longer than 230 nm [8, 4]. Other active ions included nitrite (NO_2^-) and iodine (I^-).

Ion	Concentration	Source(s)
Br^-	$840 \mu\text{M}$	[9, 10]
NO_3^-	$1.47 \mu\text{M}$	[10]
NO_2^-	$1 \mu\text{M}$	[10]
I^-	$0.5 \mu\text{M}$	[9]

Table 1: Ion makeup of modern seawater

For prebiotic seawater, optically relevant ions differ from modern abiotic seawater due

Ion	Concentration	Assumed Concentration	Source
Fe^{2+}	$10\text{-}600 \mu\text{M}$	$100 \mu\text{M}$	[11]
Br^-	$1\text{-}3 \text{ mM}$	1.5 mM	[9]
NO_3^-	$< 1 \mu\text{M}$	$1 \mu\text{M}$	[11]
Cl^-	0.5 M	0.5 M	[9]
SO_4^{2-}	$40 \mu\text{M}$	$40 \mu\text{M}$	[12]
I^-	$10\text{-}120 \mu\text{M}$	$10 \mu\text{M}$	[9]

Table 2: Ion makeup of the prebiotic ocean

to some sinks and sources of these ions being dependant on pathways driven by life. An ion known to be found in the prebiotic ocean though not in the modern ocean is ferrous iron (Fe^{2+}). The existence of ferrous iron in the prebiotic ocean is supported by banded iron formations [Figure 1], which result from the oxidisation of water-soluble ferrous iron into insoluble ferric iron (Fe^{3+}). Sulfate (SO_4^{2-}) is also known to have been found in the prebiotic ocean and reacts with ferrous iron. While sulfate is found in the modern ocean as well, in the absence of its interaction with ferrous iron, it is almost completely UV transparent on its own [12]. Ferrous iron is found to concentrations of $10\text{-}600 \mu\text{M}$, bromide to concentrations of $1\text{-}3 \text{ mM}$, and nitrate to concentrations of $1 \mu\text{M}$ or less in the prebiotic ocean [11, 4]. Our assumed concentrations for these ions can be seen in Table 2.

Once we had obtained the ion makeup of both prebiotic and modern seawater, we obtained the molar absorptivity values of the relevant ions and compounds (compounds of Fe^{2+} , NO_3^- , NO_2^- , Br^- , I^- , SO_4^{2-} , Cl^-) [13, 12, 14, 15, 16, 4]. Though bounds for the concentrations of specific ions in prebiotic seawater are found in the literature, whether ion absorbances for ferrous iron compounds could be modeled as additive was unclear. Whether the absorbance for ferrous iron compounds is additive or not plays a decisive role in the final absorbance of the prebiotic ocean. In the case of additive absorbance, the compounds ionise completely and do not interact with each other so as to affect the absorbance. This results in the total absorbance of a compound being able to be expressed as a sum of the absorbances of its component ions, as would be done with an aqueous mixture with noninteracting solutes. Whether absorbance



Figure 1: Banded iron formation. Taken from https://en.wikipedia.org/wiki/Banded_ironFormation

is additive or not is dependant on the specific compound. In order to test whether absorbances were additive for the compounds of interest ($\text{Fe}(\text{NO}_2)_2$, $\text{Fe}(\text{NO}_3)_2$, FeCl_2 , FeSO_4), we first obtained the molar absorptivity coefficient data for the listed compounds and their anions SO_4^{2-} , NO_2^- , NO_3^- , and Cl^- [13, 12, 16, 17]. The molar absorption coefficient of Fe^{2+} was taken to be that of $\text{Fe}(\text{BF}_4)_2$, the lowest of the values obtained by Fontana [13]. As all data was presented as graphs, we used Digizelt to extract the molar absorptivity coefficients. Once we had obtained the molar absorptivity coefficients from the graphs in table form, we exported this data and used it to model absorbances as additive, as presented in Equation 3.

$$\text{Total Absorbance} = \xi_{\text{ion } 1} c_{\text{ion } 1} + \xi_{\text{ion } 2} c_{\text{ion } 2} \quad (3)$$

Since the data for the molar absorptivity of the ferrous iron compounds and the molar absorptivity of the constituent anions were taken from different sources and were not at precisely the same wavelengths, the molar absorptivity values for the constituent anions were

interpolated onto the wavelength values for ferrous iron using python's interp function. This allowed the absorptivity coefficients for each ion to be evaluated at the same wavelengths. The constructed additive absorbance models were then compared to actual absorbance graphs for the compounds themselves [Figure 7, Figure 8]. We determined that absorbances for compounds of ferrous iron could not be modeled as additive.

As we found the absorbances could not be treated as additive for compounds of ferrous iron, we used the absorptivity values for the individual compounds, FeCl_2 and FeSO_4 , and not the component ions. However, as the constraints for the ion makeup of the prebiotic ocean were presented in terms of individual ions, we first had to determine the fractional abundance of the ferrous iron compounds [Table 2]. We did this by assuming equipartition, which is the reaction of ferrous iron with chloride and sulfate fractionating by the relative abundance of chloride and sulfate in the ocean. The total absorptivity contributed by all compounds of ferrous iron was considered as *oceanic ferrous iron*. We then modeled the total absorptivity for the prebiotic ocean using the values obtained for oceanic ferrous iron, nitrate, bromide, and iodide.

Certain factors did not show variance between the modern and prebiotic ocean and therefore affected our calculations in the same manner for both models. Sulfate and chloride ions, while found in both the modern and prebiotic ocean, were not included in our absorption calculation as they are not of optical significance. Sulfate and chloride are almost completely transparent in the UV in the absence of interaction with aqueous ferrous iron, which is not present to a significant degree in the modern ocean [17, 12]. However compounds of ferrous iron with sulfate and chloride were included in the absorbance of the prebiotic ocean, as these compounds are optically active. For both the prebiotic and the modern ocean, the absorptivity coefficients of pure water from Quickenden and Irvin were taken as the absorptivity coefficients of water and included in the calculation of the oceans' absorbance [3].

After we had modeled the prebiotic ocean with no organic material, in order to account for the possibility of organic material in the prebiotic ocean, we obtained molar absorptivity values for spark discharge polymers. Spark discharge polymers emerge in prebiotic Earth experiments such as the Miller-Urey experiment. These experiments assume an early Earth with a methane and ammonia rich atmosphere and provide energy to a system of such an atmosphere and water through a spark discharge. Spark discharge polymers are therefore generally accepted to be the most likely organics to have been found on prebiotic Earth. We then modeled the contribution of spark discharge polymers to UV absorption on early Earth. We varied the assumed concentration for spark discharge polymers in the prebiotic ocean by an order of magnitude starting from $1 \mu\text{M}$ in order to find the concentration at which the contribution of spark discharge polymers would become critical.

To investigate an alternate environment in which life could have emerged and contrast our models for the constructed prebiotic ocean, we modeled a sample prebiotic lake. Modern lakes are extremely diverse in their ion makeup and pH, and it is believed that prebiotic lakes shared this characteristic. We chose to construct our prebiotic lake to act as a lower bound for the UV absorption of any prebiotic lake, and therefore included only the ions that have strong support of being in all prebiotic lakes [11, 18]. These were nitrate, sulfite (SO_3^{2-}), and bisulfite (HSO_3^-). Our prebiotic lake's ion makeup can be seen in Table 3.

Ion	Concentration	Assumed Concentration
NO_3^-	$1 \mu\text{M}$	$1 \mu\text{M}$
Total sulfite	$1\text{-}1000 \mu\text{M}$	
SO_3^{2-}		$50 \mu\text{M}$
HSO_3^-	$10\text{-}120 \mu\text{M}$	$10 \mu\text{M}$

Table 3: Ion makeup of a prebiotic lake

3 Results

Our modeling of the UV transmittance for pure water revealed that pure water was almost totally UV-transparent up to ten metres, with its transmittance increasing at higher wavelengths [Figure 2]. This is in contradiction to older research values [3, 19] but in accordance with more recent literature [2]. The high UV transmission reveals that pure water on its own could not have been an effective shielder from UV light on the prebiotic Earth. Using the inverse of absorptivity to estimate the average extinction depth, we find that for wavelengths over 220 nm pure water is transmittant to 10 m, increasing to 100 m at 320 nm [Figure 3].

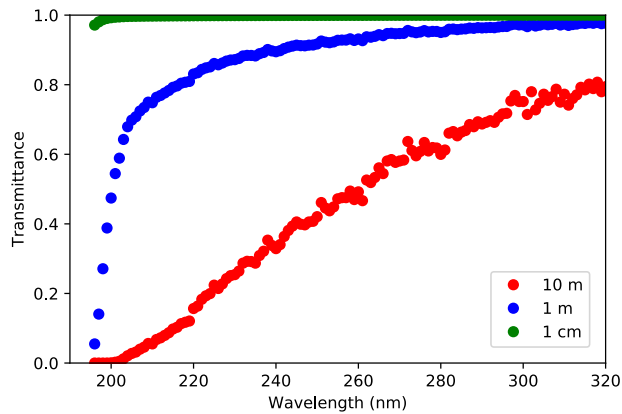


Figure 2: Transmittance of pure water based on data from [3]

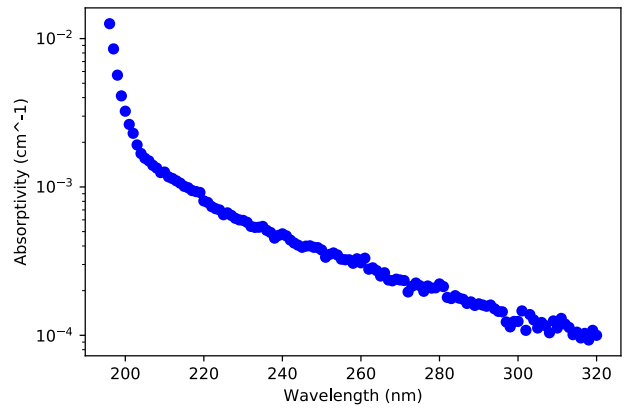


Figure 3: Absorption coefficients of pure water from [3]

For the modern abiotic ocean, we found the absorbance was dominated by bromide at wavelengths shorter than 230 nm and nitrate at wavelengths from 230 to 320 [Figure 4]. This was in accordance with the results presented by [8, 15]. The total absorbance on Figure 5 and total transmittance on Figure 6 therefore track the curve of bromide between 200-230 nm and the curve of nitrate after this, as bromide is the determining factor of absorbance for wavelengths under 230 nm and nitrate for wavelengths over 230 nm.

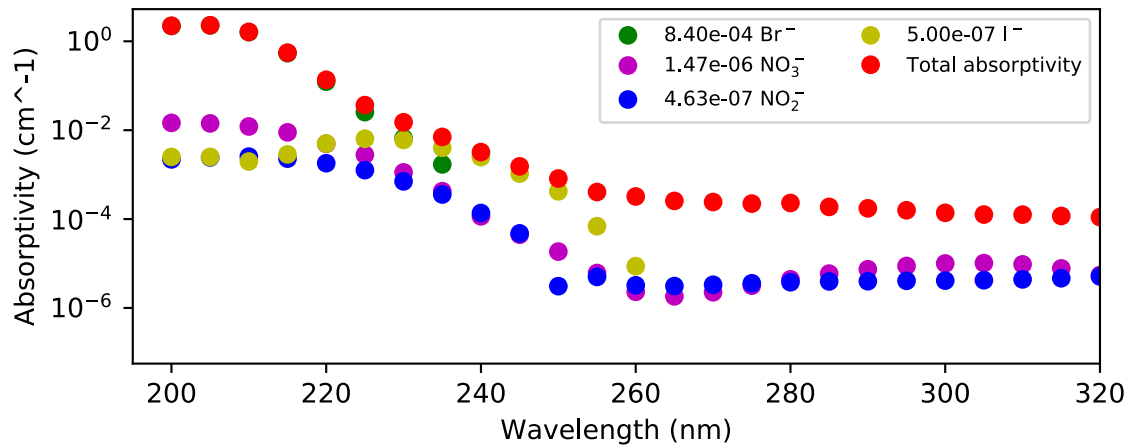


Figure 4: Absorptivities in modern oceans

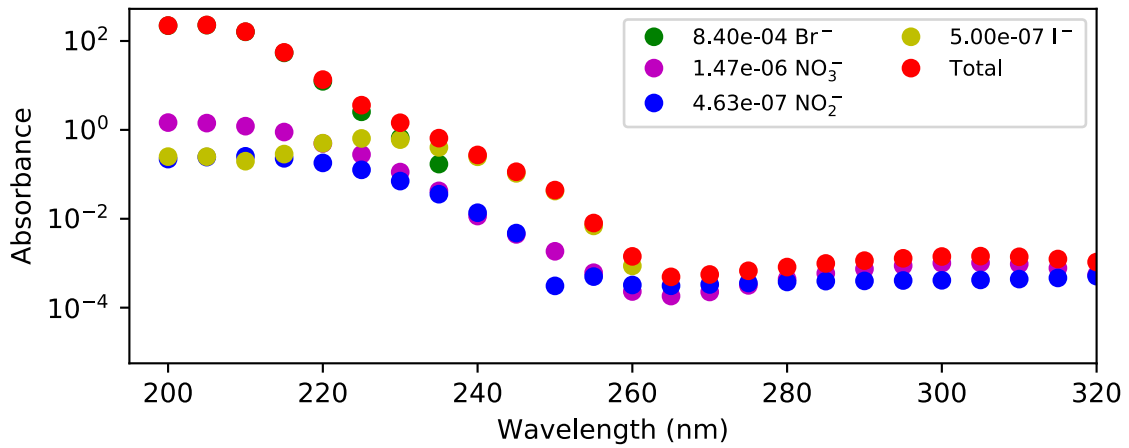


Figure 5: Absorbance in modern oceans at 100 cm

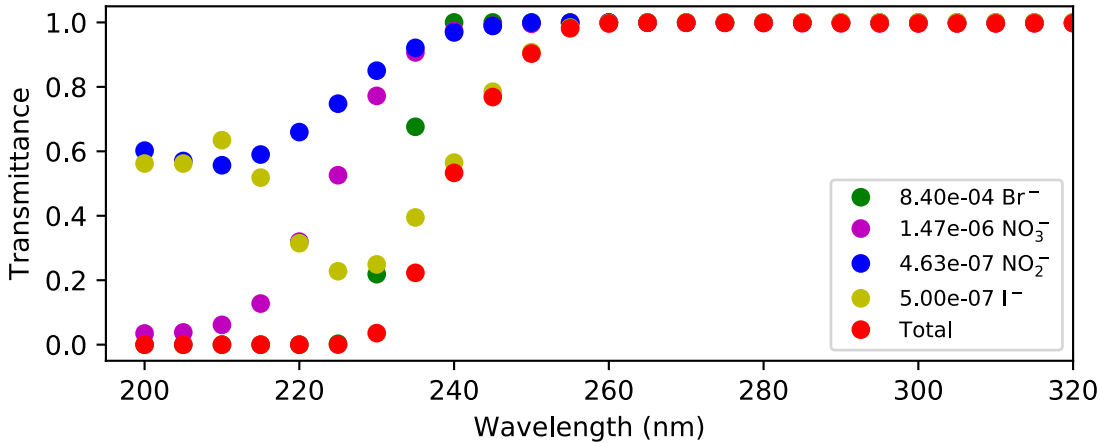


Figure 6: Transmittance in modern oceans at 100 cm

We found that the molar absorptivity values for the compounds of ferrous iron could not be treated as additive. We modeled the molar absorptivity values constructed for $FeCl_2$ and $FeSO_4$ according to Equation 3 and compared them with the molar absorptivity values given by Fontana for both the compounds of ferrous iron ($FeCl_2$ and $FeSO_4$) and $Fe(BF_4)_2$, assumed to be pure ferrous iron. If the molar absorptivities had been additive, the constructed curves would have more closely resembled the measured molar absorptivity curves for the compounds themselves, $FeCl_2$ and $FeSO_4$. However, the constructed molar absorptivity curves for both $FeCl_2$ and $FeSO_4$ closely resembled the molar absorptivity curve for $Fe(BF_4)_2$, representing pure ferrous iron [Figure 7, Figure 8]. This indicates that the absorbance for ferrous ion's compounds is dependant on ion-ion interactions and cannot be modelled in an additive manner.

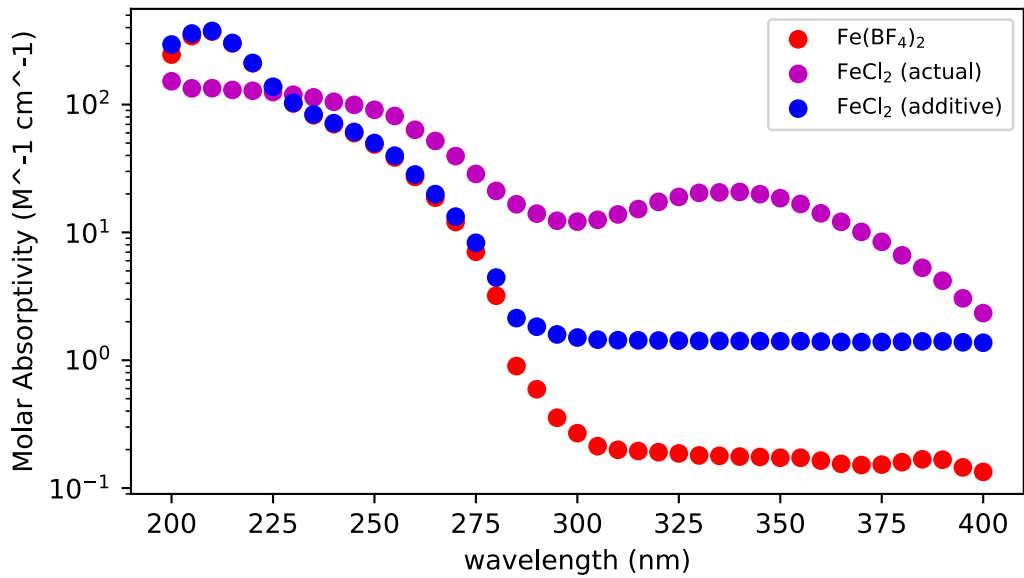


Figure 7: Constructed additive absorbance and actual molar absorbtivity curves for FeCl_2

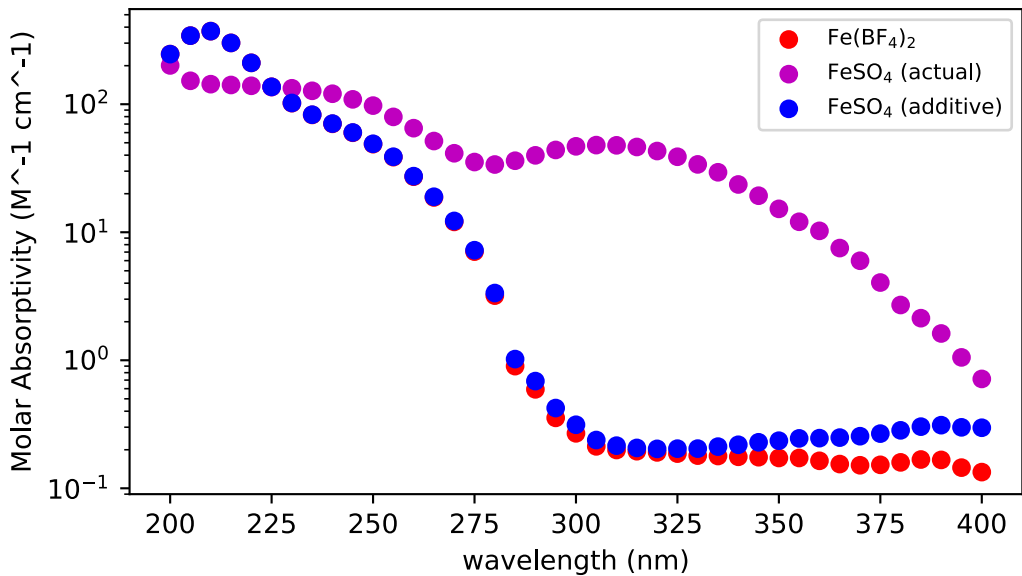


Figure 8: Constructed additive absorbance and actual molar absorbtivity curves for FeSO_4

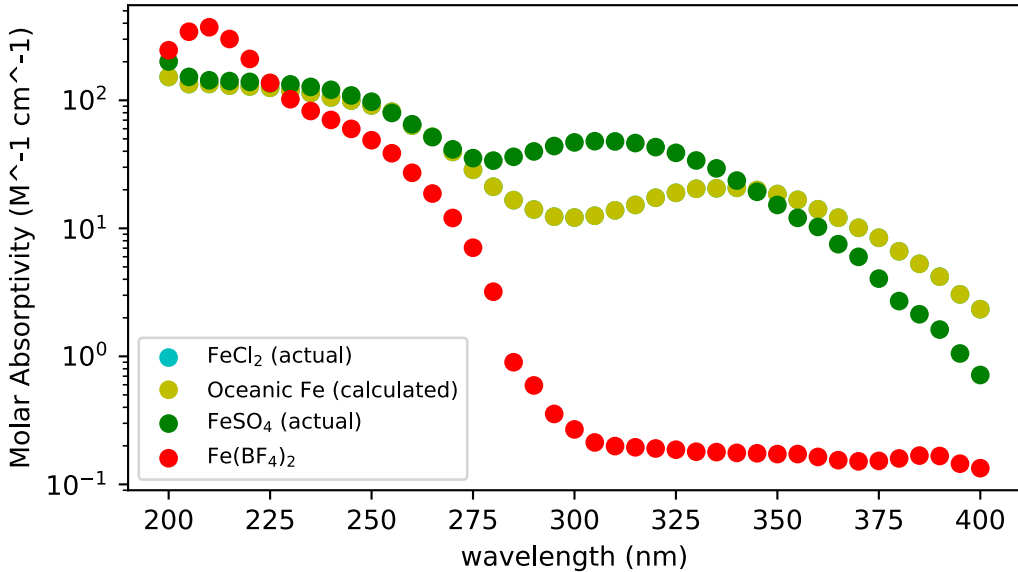


Figure 9: Constructed molar absorptivity of oceanic ferrous iron. FeCl_2 covered by oceanic iron curve

Modeling oceanic ferrous iron assuming equipartition resulted in the constructed molar absorptivity curve of oceanic ferrous iron closely tracking the measured molar absorptivity curve of FeCl_2 [Figure 9]. This was in accordance with our expectations, as the relative concentration of chloride in the prebiotic ocean is much larger than that of sulfate, their approximate molarities being $[\text{Cl}^-] = 0.5 \text{ M}$ and $[\text{SO}_4^{2-}] = 40 \mu\text{M}$ [9, 12].

We modeled the prebiotic ocean's UV environment using oceanic ferrous iron, bromide, iodide and nitrate, and found ferrous iron to be the major contributor to the UV absorbance. The second most critical contributor was iodide. The relative importance of oceanic ferrous iron and iodide can be seen in Figure 10, as their absorptivity curves carry the highest values, with the total absorptivity tracking almost exclusively onto ferrous iron after 260 nm.

Our modelling of the absorptivity of the prebiotic ocean with the contribution of the spark discharge polymer revealed that the contribution from spark discharge polymers becomes significant between the concentration of $10 \mu\text{M}$ and $100 \mu\text{M}$.

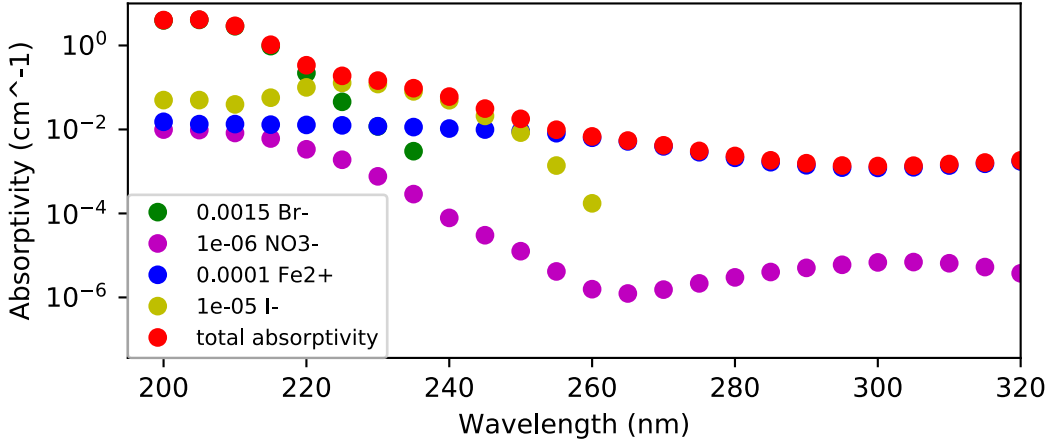


Figure 10: Absorptivities for the prebiotic ocean, no spark discharge polymer

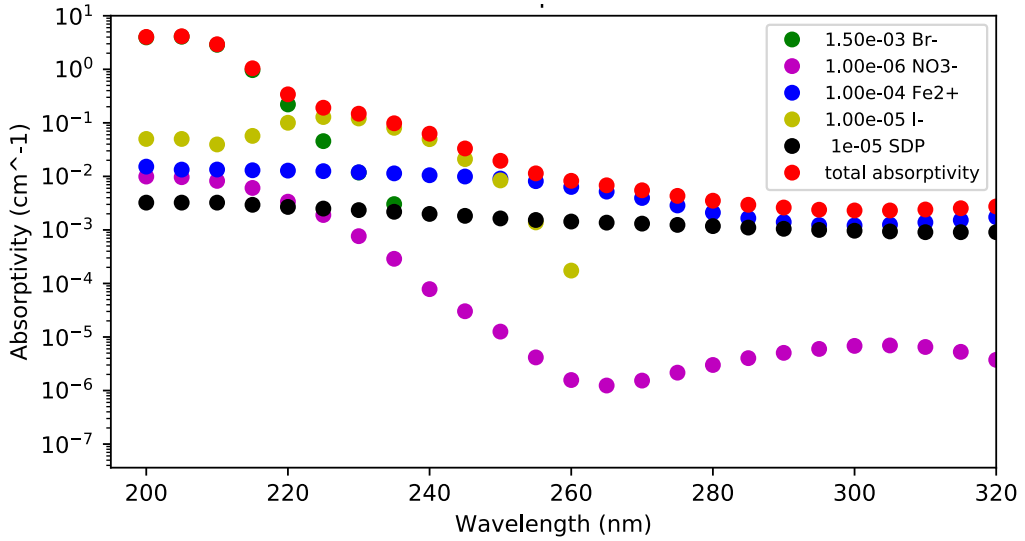


Figure 11: Absorptivities in the prebiotic ocean with $10 \mu\text{M}$ spark discharge polymer (SDP)

We compared the prebiotic ocean's UV environment to modern abiotic ocean water, the clearest ocean waters, and a prebiotic lake, and found that upwards of 250 nm, the prebiotic ocean is less UV transmittant than both the constructed modern abiotic ocean and the clearest waters [7]. The absorptivities we have found for the prebiotic ocean reveal that at wavelengths under 210 nm, UV extinction occurs at 1 cm. The extinction depth approaches 10 m as the wavelength approaches 320 nm.

We found that our prebiotic lake was to some degree more UV-transparent than the prebiotic ocean and less transparent than the modern abiotic ocean [Figure 13]. The prebiotic lake we modeled was UV transparent to 0.8 at 1 m. This high transmittance indicates that it is possible for prebiotic lakes and ponds to have been almost completely UV-transparent to their full depth.

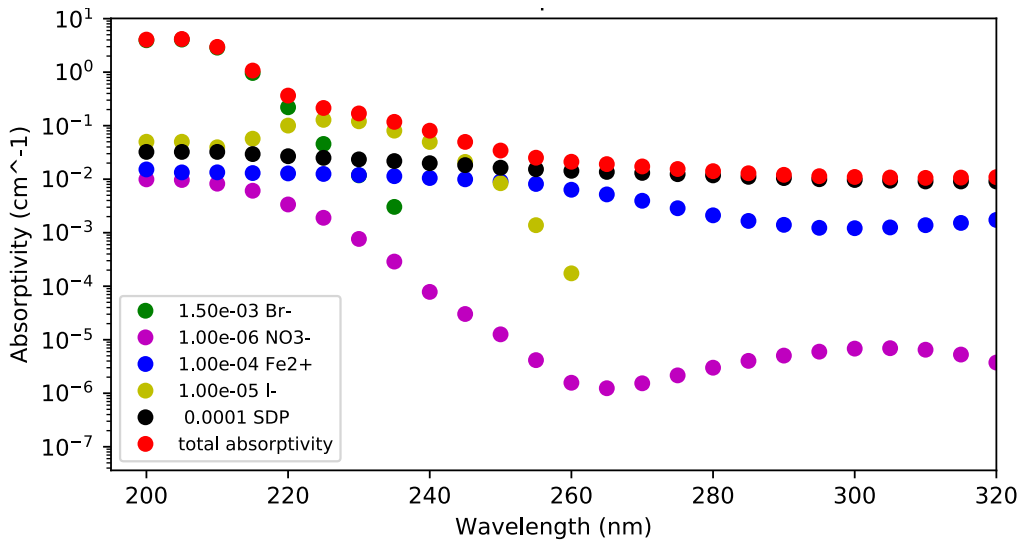


Figure 12: Absorptivities in the prebiotic ocean with $100 \mu\text{M}$ spark discharge polymer (SDP)

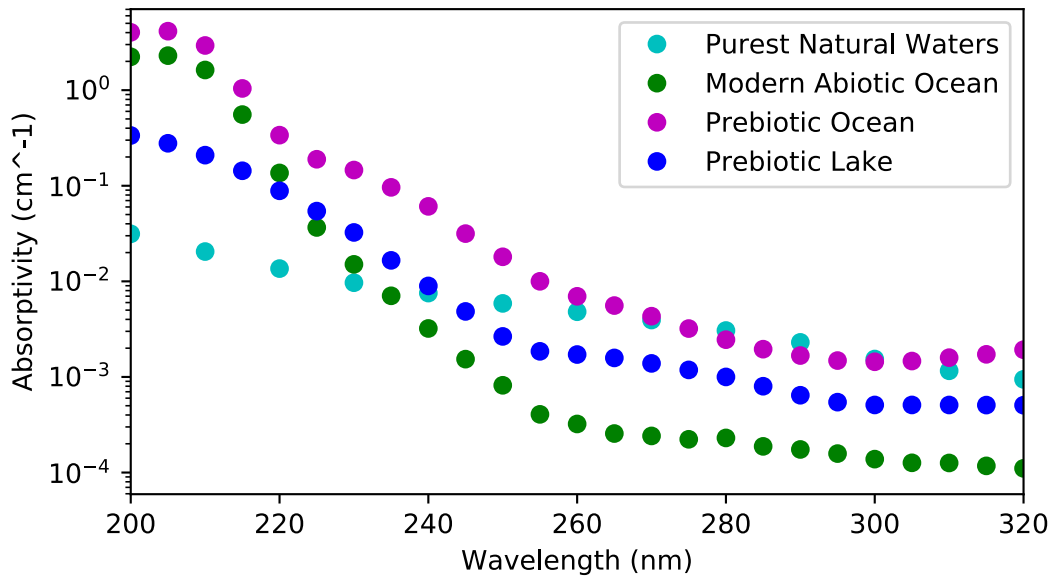


Figure 13: Absorptivities of modern abiotic ocean, prebiotic ocean, clearest ocean waters and prebiotic lake

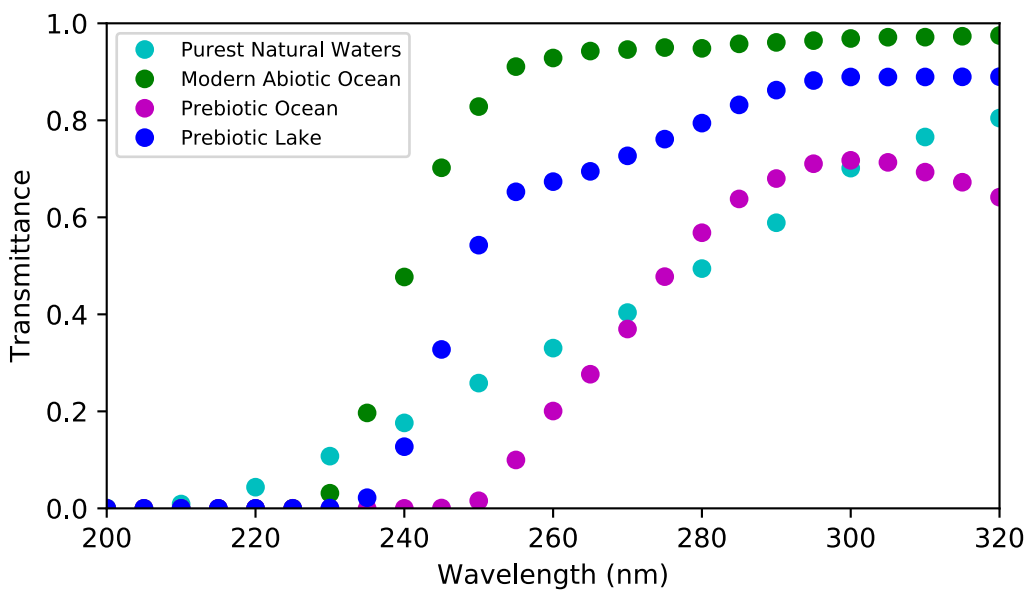


Figure 14: Transmittance of modern abiotic ocean, prebiotic ocean, clearest ocean waters and prebiotic lake at 1 m

4 Discussion

The values we have found for the extinction depth of UV light in the prebiotic ocean reveal that appreciable energy could have only been delivered to the first 10 m of the prebiotic ocean by UV light. At depths below this, any biotic molecules would be shielded from UV damage. Conversely, UV light would have only been a viable source of energy for photochemical reactions in the topmost 10 m layer. In the case of biotic molecules being produced only in this layer, they would dissipate throughout the ocean into larger depths, likely resulting in extremely low concentrations of such molecules. The dissipation and subsequent low concentration leads to the problem of biotic molecules being less likely to engage in reactions leading to origin of life pathways. This is due to the reaction rate of any chemical reaction being tied to the concentration of its reactants. With a decrease in the concentration of reactants, as seen in dissipation, a decrease in the rate of reaction occurs as molecules are less likely to collide and therefore less likely to engage in successful reactions.

We find that certain prebiotic lakes would have been slightly less UV transparent than the prebiotic ocean, though still UV transparent up to 80% at wavelengths higher than 250 nm at 1 m. It is important to point out that the vast majority of prebiotic lakes would have been more absorbant in the UV than our model, as we included only the base amount of ions known to have been present in prebiotic lakes and not any other dissolved geological matter. Our results for the UV transmission of prebiotic lakes are in contradiction to the findings of Pearce et al., who state at a depth of 1 m, lake water could absorb 95% of UV irradiation [4]. Our result of 80% transmittance or 20% absorbance for a prebiotic lake with minimal absorbant material leads us to conclude Pearce et al.'s conclusion is not true for all lakes, but rather depends on the composition of the individual lake. Pearce et al.'s pathway for RNA polymerisation in warm little ponds should therefore be regarded as possible in a subset of prebiotic ponds and not universally applicable to prebiotic ponds.

In this work, we have modeled the UV absorbances of modern abiotic seawater and the prebiotic ocean using previous experimental data. Further experimental work that may be used to test these models include the construction of modern abiotic seawater and prebiotic seawater in the laboratory according to Table 1 and Table 2 and then conducting spectrophotometry of these solutions. The same procedure may be followed for our prebiotic lake. In addition, different ions possible to have been found on early Earth could be added to the ions we used to model the prebiotic lake in order to diversify prebiotic lake conditions on which there are constraints [Table 3].

In constructing our absorption model for the prebiotic ocean, we have assumed equipartition of the FeCl_2 and FeSO_4 reactions. We believe this estimation to be accurate to the first order. A more accurate estimation might be reached by using the stability constants for these compounds.

We have identified that the absorption contributed by organics, which we evaluated in the form of spark discharge polymers, would become significant between 10 and 100 μM . Further work might investigate the likely concentration of such polymers in prebiotic lakes.

Our model of the modern abiotic, prebiotic, and modern clearest ocean waters reveal that modern abiotic seawater is more absorbent than clearest ocean waters at wavelengths below 230 nm. Although this is not in accordance with our expectations, as the clearest ocean water should include the absorbent factors in abiotic seawater along with the minimal organic factors, Smith and Baker state that their values under 300 nm are merely educated guesses [7]. We also find that modern abiotic seawater is more transparent in the UV than prebiotic seawater. This should be taken into account along with the higher availability of UV on early Earth in evaluating origin of life scenarios in the prebiotic ocean.

5 Acknowledgments

Special thanks goes to Dr. Sukrit Ranjan for his mentorship and guidance in this research. I would also like to thank Dr. Jenny Sendova for her tutoring and help throughout RSI and the writing of this paper. I thank Dr. Clara Sousa-Silva for her kind support during the conducting of this study, and Hangyul Lyna Kim for her help in revising this paper. Finally, I thank Subor Boru Sanayi Vetic for sponsoring me, and the Research Science Institute, the Center for Excellence in Education and the Massachusetts Institute of Technology for this opportunity.

References

- [1] G. E. Thomas and K. Stamnes. *Radiative transfer in the atmosphere and ocean*. Cambridge University Press, 2002.
- [2] S. Ranjan and D. D. Sasselov. Influence of the uv environment on the synthesis of prebiotic molecules. *Astrobiology*, 16(1):68–88, 2016.
- [3] T. Quickenden and J. Irvin. The ultraviolet absorption spectrum of liquid water. *The Journal of Chemical Physics*, 72(8):4416–4428, 1980.
- [4] B. K. Pearce, R. E. Pudritz, D. A. Semenov, and T. K. Henning. Origin of the rna world: The fate of nucleobases in warm little ponds. *Proceedings of the National Academy of Sciences*, 114(43):11327–11332, 2017.
- [5] J. Farquhar, H. Bao, and M. Thiemens. Atmospheric influence of earth’s earliest sulfur cycle. *Science*, 289(5480):756–758, 2000.
- [6] A. Pavlov and J. Kasting. Mass-independent fractionation of sulfur isotopes in archean sediments: strong evidence for an anoxic archean atmosphere. *Astrobiology*, 2(1):27–41, 2002.
- [7] R. C. Smith and K. S. Baker. Optical properties of the clearest natural waters (200–800 nm). *Applied optics*, 20(2):177–184, 1981.
- [8] Y. Collos, F. Mornet, A. Sciandra, N. Waser, A. Larson, and P. Harrison. An optical method for the rapid measurement of micromolar concentrations of nitrate in marine phytoplankton cultures. *Journal of Applied Phycology*, 11(2):179–184, 1999.
- [9] D. D. Channer, C. De Ronde, and E. Spooner. The cl- br- i- composition of 3.23 ga modified seawater: implications for the geological evolution of ocean halide chemistry. *Earth and Planetary Science Letters*, 150(3-4):325–335, 1997.
- [10] <http://img.21food.cn/img/biaozhun/20090815/187/11183599.pdf>.
- [11] S. Ranjan, Z. R. Todd, P. B. Rimmer, D. D. Sasselov, and A. R. Babbin. Nitrogen oxide concentrations in natural waters on early earth. *Geochemistry, Geophysics, Geosystems*, 20(4):2021–2039, 2019.
- [12] E. Hayon and J. J. McGarvey. Flash photolysis in the vacuum ultraviolet region of sulfate, carbonate, and hydroxyl ions in aqueous solutions. *The Journal of Physical Chemistry*, 71(5):1472–1477, 1967.
- [13] I. Fontana, A. Lauria, and G. Spinolo. Optical absorption spectra of fe²⁺ and fe³⁺ in aqueous solutions and hydrated crystals. *physica status solidi (b)*, 244(12):4669–4677, 2007.

- [14] K. S. Johnson and L. J. Coletti. In situ ultraviolet spectrophotometry for high resolution and long-term monitoring of nitrate, bromide and bisulfide in the ocean. *Deep Sea Research Part I: Oceanographic Research Papers*, 49(7):1291–1305, 2002.
- [15] E. A. Guenther, K. S. Johnson, and K. H. Coale. Direct ultraviolet spectrophotometric determination of total sulfide and iodide in natural waters. *Analytical Chemistry*, 73(14):3481–3487, 2001.
- [16] J. Mack and J. R. Bolton. Photochemistry of nitrite and nitrate in aqueous solution: a review. *Journal of Photochemistry and Photobiology A: Chemistry*, 128(1-3):1–13, 1999.
- [17] H.-H. Perkampus. *UV-VIS Spectroscopy and its Applications*. Springer Science & Business Media, 2013.
- [18] S. Ranjan, Z. R. Todd, J. D. Sutherland, and D. D. Sasselov. Sulfidic anion concentrations on early earth for surficial origins-of-life chemistry. *Astrobiology*, 18(8):1023–1040, 2018.
- [19] H. J. Cleaves and S. L. Miller. Oceanic protection of prebiotic organic compounds from uv radiation. *Proceedings of the National Academy of Sciences*, 95(13):7260–7263, 1998.

Appendix A Python Code for Modelling the Modern Abiotic Ocean

```
1 #!/usr/bin/env python3
2 # -*- coding: utf-8 -*-
3 """
4 Created on Fri Jul 26 15:26:26 2019
5 @author: azrahaseki
6 """
7
8 #importing important libraries
9 import matplotlib.pyplot as plt
10 import numpy as np
11 import pdb
12
13 s = 100 #depth in units of cm
14
15 #specifiying modern concentrations of ions
16 M_br_mod = 0.000840 #840 uM
17 M_no3_mod = 0.00000147 #1.470 uM
18 M_no2_mod = 0.000000463 #1 uM
19 M_i_mod = 0.0000005 #0.5 uM
20
21 #importing data
22 wv_br, molabs_br = np.genfromtxt('./Processed-Data/johnson_br.dat', skip_header=2, \
```

```

23 unpack=True, usecols=(0,1)) #nm, M^=1 cm^-1..
24 wv_febf4, molabs_febf4 = np.genfromtxt('./Processed-Data/fontana_fe2bf4.dat', \
25 skip_header=2, unpack=True, usecols=(0,1)) #nm, M^=1 cm^-1
26 wv_i, molabs_i = np.genfromtxt('./Processed-Data/guenther_i.dat', skip_header=2, \
27 unpack=True, usecols=(0,1)) #nm, M^=1 s^-1,
28 wv_no2, molabs_no2 = np.genfromtxt('./Processed-Data/mack_no2.dat', skip_header=2, \
29 unpack=True, usecols=(0,1)) #nm, M^=1 cm^-1...
30 wv_no3, molabs_no3 = np.genfromtxt('./Processed-Data/mack_no3.dat', skip_header=2, \
31 unpack=True, usecols=(0,1)) #nm, M^=1 cm^-1
32
33 wv_quickenden, molabs_quickenden = np.genfromtxt('./Processed-Data/quickenden.dat', \
34
35 skip_header=2, unpack=True, usecols=(0,1)) #nm, M^=1
36
37
38 #interpolating to Fe wavelength
39 molabs_br_adjusted = np.interp(wv_febf4, wv_br, molabs_br)
40 molabs_no3_adjusted = np.interp(wv_febf4, wv_no3, molabs_no3)
41 molabs_i_adjusted = np.interp(wv_febf4, wv_i, molabs_i)
42 molabs_no2_adjusted = np.interp(wv_febf4, wv_no2, molabs_no2)
43 molabs_quickenden_adjusted = np.interp(wv_febf4, wv_quickenden, molabs_quickenden)
44
45 def calculate_modern_ocean():
46     return (molabs_br_adjusted * M_br_mod + molabs_no3_adjusted * M_no3_mod + \
47             molabs_no2_adjusted * M_no2_mod + molabs_i_adjusted * M_i_mod + \
48             molabs_quickenden_adjusted) #calculating molar absorptivity of the modern ocean

```

```

49

50 modern_absorptivity = calculate_modern_ocean()

51 np.savetxt("./Processed-Data/constructed_modern_ocean.dat", \
52 np.column_stack((wv_febf4, modern_absorptivity)), delimiter=",", newline="\n", \
53 fmt="%3.1f %1.6e", header="Constructed molar absorbtivity of the modern \
54 ocean\nWavelength (nm), Absorptivities (cm^-1)")

55

56 #calculating absorbances

57 absorbance_br = molabs_br_adjusted * M_br_mod * s

58 absorbance_no3 = molabs_no3_adjusted * M_no3_mod * s

59 absorbance_no2 = molabs_no2_adjusted * M_no2_mod * s

60 absorbance_i = molabs_i_adjusted * M_i_mod * s

61 absorbance_total = absorbance_br + absorbance_no3 + absorbance_no2 + absorbance_i

62

63 #calculating transmittances

64 trans_br = 10 ** (-1 * absorbance_br)

65 trans_no3 = 10 ** (-1 * absorbance_no3)

66 trans_no2 = 10 ** (-1 * absorbance_no2)

67 trans_i = 10 ** (-1 * absorbance_i)

68 trans_total = 10 ** (-1 * absorbance_total)

69

70 #calculating total absorptivity for modern ocean

71 absorptivity_total = molabs_quickenden_adjusted + molabs_br_adjusted * M_br_mod \
72 + molabs_no3_adjusted * M_no3_mod + molabs_no2_adjusted * M_no2_mod + \
73 molabs_i_adjusted * M_i_mod

74 #saving absorptivity for the modern ocean

```

```

75 #np.savetxt("./Processed-Data/constructed_modern_ocean.dat", \
76 np.column_stack((wv_febf4, absorptivity_total)), delimiter=",", newline="\n", \
77 fmt="%3.1f %1.6e", header="Constructed molar absorbtivity of the modern \
78 ocean\nWavelength (nm), Absorptivities (cm^-1)")

79

80 ##### graphing the modern ocean #####
81 fig, axes = plt.subplots(4,figsize=(6.5,12.))

82

83 #graphing molar absorptivities

84 axes[0].plot(wv_febf4, molabs_br_adjusted, "go", label="Br$^-$")
85 axes[0].plot(wv_febf4, molabs_no3_adjusted, "mo", label="NO$_3^-$")
86 axes[0].plot(wv_febf4, molabs_no2_adjusted, "bo", label="NO$_2^-$")
87 axes[0].plot(wv_febf4, molabs_i_adjusted, "yo", label="I$^-")

88

89 axes[0].set_xlabel("Wavelength (nm) #titling x axis"
90 axes[0].set_ylabel("Molar Absorptivity (M^-1 cm^-1) #titling y axis"
91 axes[0].set_title("Molar Absorbtivities")
92 axes[0].legend(loc="best", ncol=2,borderaxespad=0.5, fontsize=8) #creating legend
93 axes[0].set_yscale("log")
94 axes[0].set_xlim([195,320])

95

96 #graphing absorptivities

97 axes[1].plot(wv_febf4, molabs_br_adjusted * M_br_mod, "go", \
98 label=".2e Br$^-$ % (M_br_mod)")
99 axes[1].plot(wv_febf4, molabs_no3_adjusted * M_no3_mod, "mo", \
100 label=".2e NO$_3^-$ % (M_no3_mod)")

```

```

101 axes[1].plot(wv_febf4, molabs_no2_adjusted * M_no2_mod, "bo", \
102 label=".2e NO$_2$-%(M_no2_mod))"
103 axes[1].plot(wv_febf4, molabs_i_adjusted * M_i_mod, "yo", \
104 label=".2e I$-$-%(M_i_mod))"
105 axes[1].plot(wv_febf4, absorptivity_total, "ro", label="Total absorptivity")
106
107 axes[1].set_xlabel("Wavelength (nm)" ) #titling x axis
108 axes[1].set_ylabel("Absorptivity (cm^-1)" ) #titling y axis
109 axes[1].set_title("Absorptivities")
110 axes[1].legend(loc="best", ncol=2,borderaxespad=0.5, fontsize=7.5) #creating legend
111 axes[1].set_yscale("log")
112 axes[1].set_xlim([195,320])
113
114 #graphing absorbance
115 axes[2].plot(wv_febf4, absorbance_br, "go", label=".2e Br$-$-%(M_br_mod))
116 axes[2].plot(wv_febf4, absorbance_no3, "mo", label=".2e NO$_3$-$-%(M_no3_mod))")
117 axes[2].plot(wv_febf4, absorbance_no2, "bo", label=".2e NO$_2$-$-%(M_no2_mod))")
118 axes[2].plot(wv_febf4, absorbance_i, "yo", label=".2e I$-$-%(M_i_mod))")
119 axes[2].plot(wv_febf4, absorbance_total, "ro", label="Total")
120
121 axes[2].set_xlabel("Wavelength (nm)" ) #titling x axis
122 axes[2].set_ylabel("Absorbance" ) #titling y axis
123 axes[2].set_title("Absorbance at %s cm" %(s))
124 axes[2].legend(loc="best", ncol=2,borderaxespad=0.5, fontsize=8) #creating legend
125 axes[2].set_yscale("log")
126 axes[2].set_xlim([195,320])

```

```

127
128
129 #graphing transmittance
130 axes[3].plot(wv_febf4, trans_br, "go", label=".2e Br$^-$ %(M_br_mod)")
131 axes[3].plot(wv_febf4, trans_no3, "mo", label=".2e NO$_3^-$ %(M_no3_mod))
132 axes[3].plot(wv_febf4, trans_no2, "bo", label=".2e NO$_2^-$ %(M_no2_mod))
133 axes[3].plot(wv_febf4, trans_i, "yo", label=".2e I$^-$ %(M_i_mod))
134 axes[3].plot(wv_febf4, trans_total, "ro", label="Total")
135
136 axes[3].set_xlabel("Wavelength (nm) #titling x axis"
137 axes[3].set_ylabel("Transmittance") #titling y axis
138 axes[3].set_title("Transmittance at %s cm" %(s))
139 axes[3].legend(loc="best", ncol=1, borderaxespad=0.5, fontsize=8) #creating legend
140 #axes[2].set_yscale("log")
141 axes[3].set_xlim([195,320])
142
143
144 plt.subplots_adjust(left=0.125, bottom=0.1, right=0.9, top=0.9, wspace=0.01, \
145 hspace=0.4) #adjusting spacing
146 plt.savefig("Modern_Ocean.pdf", orientation="portrait", papertype='letter', \
147 format="pdf") #saving graph as pdf
148 plt.show() #display graph##

```

Appendix B Python Code for Modelling the Prebiotic Ocean

```
1      #!/usr/bin/env python3
2  # -*- coding: utf-8 -*-
3  """
4  Created on Mon Jul 22 11:41:21 2019
5
6  @author: azrahaseki
7
8  legend: molabs_ion: the molar absorptivity constants (in M^-1 cm^-1) for that ion.
9  """
10
11 #importing important libraries
12 import matplotlib.pyplot as plt
13 import numpy as np
14 import pdb
15
16 s = 100 #depth in units of cm
17
18 #specifying prebiotic concentrations of ions
19 M_fe_prebio = 0.000100 #10-600 uM
20 M_br_prebio = 0.0015 #1-3 mM
21 M_no3_prebio = 0.000001 #maximum 1 uM
22 M_fecl2_prebio = 0.00001
```

```

23 M_feso4_prebio = 0.00001
24 M_i_prebio = 0.00001 #10-120 uM
25 M_gelbstoff_prebio = 0.0001 #experimenting #1 uM
26
27 #specifying modern concentrations of ions
28 M_br_mod = 0.000840 #840 uM
29 M_no3_mod = 0.00000147 #1.470 uM
30 M_no2_mod = 0.000000463 #1 uM
31 M_i_mod = 0.0000005 #0.5 uM
32
33 #importing data
34 wv_br, molabs_br = np.genfromtxt('./Processed-Data/johnson_br.dat', \
35 skip_header=2, unpack=True, usecols=(0,1)) #nm, M^=1 cm^-1...
36 wv_febf4, molabs_febf4 = np.genfromtxt('./Processed-Data/fontana_fe2bf4.dat', \
37 skip_header=2, unpack=True, usecols=(0,1)) #nm, M^=1 cm^-1
38 wv_fecl2, molabs_fecl2 = np.genfromtxt('./Processed-Data/fontana_fecl2.dat', \
39 skip_header=2, unpack=True, usecols=(0,1)) #nm, M^=1 cm^-1...
40 wv_feso4, molabs_feso4 = np.genfromtxt('./Processed-Data/fontana_feso4.dat', \
41 skip_header=2, unpack=True, usecols=(0,1)) #nm, M^=1 cm^-1...
42 wv_cl, molabs_cl = np.genfromtxt('./Processed-Data/perkampus_kcl.dat', \
43 skip_header=2, unpack=True, usecols=(0,1)) #nm, M^=1 s^-1
44 #wv_so4, molabs_so4 = np.genfromtxt('./Processed-Data/hayon_so4_acid.dat', \
45 skip_header=2, unpack=True, usecols=(0,1)) #nm, M^=1 s^-1,
46 wv_so4, molabs_so4 = np.genfromtxt('./Processed-Data/hayon_so4_base.dat', \
47 skip_header=2, unpack=True, usecols=(0,1)) #nm, M^=1 s^-1,
48 wv_i, molabs_i = np.genfromtxt('./Processed-Data/guenther_i.dat', \

```

```

49 skip_header=2, unpack=True, usecols=(0,1)) #nm, M^-1 s^-1,
50 wv_no2, molabs_no2 = np.genfromtxt('./Processed-Data/mack_no2.dat', \
51 skip_header=2, unpack=True, usecols=(0,1))#nm, M^-1 cm^-1...
52 wv_no3, molabs_no3 = np.genfromtxt('./Processed-Data/mack_no3.dat', \
53 skip_header=2, unpack=True, usecols=(0,1))#nm, M^-1 cm^-1
54 wv_gelbstoff, molabs_gelbstoff = np.genfromtxt('./Processed-Data/cleaves_gelbstoff.dat' \
55 , skip_header=2, unpack=True, usecols=(0,1))#nm, M^-1 cm^-1
56
57 wv_pure, molabs_pure = np.genfromtxt('./Processed-Data/smithbaker_purest.dat' \
58 , skip_header=2, unpack=True, usecols=(0,1))#nm, M^-1
59 wv_quickenden, molabs_quickenden = np.genfromtxt('./Processed-Data/quickenden.dat', \
60 skip_header=2, unpack=True, usecols=(0,1))#nm, M^-1
61
62 #calculating synthetic absorptivities
63 molabs_fecl2_synthetic=molabs_febf4 + 2.0*np.interp(wv_febf4, wv_cl, molabs_cl) \
64 #M^-1 cm^-1
65 molabs_feso4_synthetic=molabs_febf4 + np.interp(wv_febf4, wv_so4, molabs_so4) \
66 #M^-1 cm^-1
67
68
69 #interpolating to Fe wavelength
70 molabs_br_adjusted = np.interp(wv_febf4, wv_br, molabs_br)
71 molabs_no3_adjusted = np.interp(wv_febf4, wv_no3, molabs_no3)
72 molabs_i_adjusted = np.interp(wv_febf4, wv_i, molabs_i)
73 molabs_pure_adjusted = np.interp(wv_febf4, wv_pure, molabs_pure)
74 molabs_no2_adjusted = np.interp(wv_febf4, wv_no2, molabs_no2)

```

```

75 molabs_quickenden_adjusted = np.interp(wv_febf4, wv_quickenden, molabs_quickenden)
76 molabs_gelbstoff_adjusted = np.interp(wv_febf4, wv_gelbstoff, molabs_gelbstoff)
77
78
79
80 def calculate_fe_oceanic(fecl2_to_feso4_ratio):
81     """
82     Takes: ratio of Fe in FeCl2 vs Fe in FeSO4 \
83     (expected to be high since much more Cl than SO4)
84     """
85     return ((fecl2_to_feso4_ratio)/(1.0+fecl2_to_feso4_ratio))*molabs_fecl2 + \
86             ((1.0)/(1.0+fecl2_to_feso4_ratio))*np.interp(wv_fecl2, wv_feso4, molabs_feso4)
87
88 molabs_fe_oceanic=calculate_fe_oceanic(0.5/(40.0e-6)) #calculating "constructed" \
89 molar absorbtivity of Fe2+
90 np.savetxt("./Processed-Data/constructed_Fe_molarabsorptivity.dat", \
91 np.column_stack((wv_fecl2, molabs_fe_oceanic)), delimiter=",", newline="\n", \
92 fmt="%3.1f %1.6e", header="Constructed molar absorbtivity of Fe2+ in the prebiotic \
93 ocean\nWavelength (nm), Molar Absorptivities (M-1 cm-1)")
94
95 def calculate_modern_ocean():
96     return (molabs_br_adjusted * M_br_mod + molabs_no3_adjusted * M_no3_mod + \
97             molabs_no2_adjusted * M_no2_mod + molabs_i_adjusted * M_i_mod + \
98             molabs_quickenden_adjusted) #calculating molar absorptivity of the modern ocean
99
100 modern_absorptivity = calculate_modern_ocean()

```

```

101 np.savetxt("./Processed-Data/constructed_modern_ocean.dat", \
102 np.column_stack((wv_febf4, modern_absorptivity)), delimiter=",", newline="\n", \
103
104 fmt="%3.1f %1.6e", header="Constructed molar absorbtivity of the modern \
105 ocean\nWavelength (nm), Absorptivities (cm^-1)")
106
107 #calculating absorbances
108 absorbance_br = molabs_br_adjusted * M_br_prebio * s
109 absorbance_no3 = molabs_no3_adjusted * M_no3_prebio * s
110 absorbance_fe = molabs_fe_oceanic * M_fe_prebio * s
111 absorbance_i = molabs_i_adjusted * M_i_prebio * s
112 absorbance_gelbstoff = molabs_gelbstoff_adjusted * M_gelbstoff_prebio * s
113 absorbance_total = absorbance_br + absorbance_no3 + absorbance_fe + absorbance_i \
114 + absorbance_gelbstoff
115
116 #calculating transmittances
117 trans_br = 10 ** (-1 * absorbance_br)
118 trans_no3 = 10 ** (-1 * absorbance_no3)
119 trans_fe = 10 ** (-1 * absorbance_fe)
120 trans_i = 10 ** (-1 * absorbance_i)
121 trans_gelbstoff = 10 ** (-1 * absorbance_gelbstoff)
122 trans_total = 10 ** (-1 * absorbance_total)
123
124 #calculating total absorptivity for prebiotic ocean
125 absorptivity_total = molabs_quickenden_adjusted + molabs_br_adjusted * M_br_prebio \
126 + molabs_no3_adjusted * M_no3_prebio + molabs_fe_oceanic * M_fe_prebio + \

```

```

127 molabs_i_adjusted * M_i_prebio + molabs_gelbstoff_adjusted * M_gelbstoff_prebio
128 np.savetxt("./Processed-Data/constructed_prebiotic_ocean.dat", \
129 np.column_stack((wv_febf4, absorptivity_total)), delimiter=",", newline="\n", \
130 fmt="%3.1f %1.6e", header="Constructed molar absorbtivity of the prebiotic \
131 ocean\nWavelength (nm), Absorptivities (cm^-1)")
132
133 ##### graphing the prebiotic ocean #####
134 fig, axes = plt.subplots(4,figsize=(7,18.))
135
136 #graphing molar absorptivities
137 axes[0].plot(wv_febf4, molabs_br_adjusted, "go", label="Br-")
138 axes[0].plot(wv_febf4, molabs_no3_adjusted, "mo", label="NO3-")
139 axes[0].plot(wv_fecl2, molabs_fe_oceanic, "bo", label="Oceanic Fe (simulated)")
140 axes[0].plot(wv_fecl2, molabs_gelbstoff_adjusted, "ko", \
141 label="Hydrogen Discharge Polymer")
142 axes[0].plot(wv_fecl2, molabs_i_adjusted, "yo", label="I-")
143
144 axes[0].set_xlabel("Wavelength (nm)") #titling x axis
145 axes[0].set_ylabel("Molar Absorptivity (M^-1 cm^-1)") #titling y axis
146 axes[0].set_title("Molar Absorbtivities")
147 axes[0].legend(loc="best", ncol=1,borderaxespad=0, fontsize=8) #creating legend
148 axes[0].set_yscale("log")
149 axes[0].set_xlim([195,320])
150
151 #graphing absorptivities
152 axes[1].plot(wv_febf4, molabs_br_adjusted * M_br_prebio, "go", \

```

```

153 label=".2e Br- " %(M_br_prebio))

154 axes[1].plot(wv_febf4, molabs_no3_adjusted * M_no3_prebio, "mo", \
155 label=".2e NO3- " %(M_no3_prebio))

156 axes[1].plot(wv_fecl2, molabs_fe_oceanic * M_fe_prebio, "bo", \
157 label=".2e Fe2+ " %(M_fe_prebio))

158 axes[1].plot(wv_fecl2, molabs_i_adjusted * M_i_prebio, "yo", \
159 label=".2e I- " %(M_i_prebio))

160 axes[1].plot(wv_fecl2, molabs_gelbstoff_adjusted * M_gelbstoff_prebio, "ko", \
161 label="%s SDP" %(M_gelbstoff_prebio))

162 axes[1].plot(wv_fecl2, absorptivity_total, "ro", label="total absorptivity")

163

164 axes[1].set_xlabel("Wavelength (nm)" ) #titling x axis
165 axes[1].set_ylabel("Absorptivity (cm^-1)" ) #titling y axis
166 axes[1].set_title("Absorptivities")
167 axes[1].legend(loc="best", ncol=1,borderaxespad=0.5, fontsize=8) #creating legend
168 axes[1].set_yscale("log")
169 axes[1].set_xlim([195,320])

170

171 #graphing absorbance

172 axes[2].plot(wv_febf4, absorbance_br, "go", label=".2e Br- " %(M_br_prebio))
173 axes[2].plot(wv_febf4, absorbance_no3, "mo", label=".2e NO3- " %(M_no3_prebio))
174 axes[2].plot(wv_febf4, absorbance_fe, "bo", label=".2e Fe2+ " %(M_fe_prebio))
175 axes[2].plot(wv_febf4, absorbance_i, "yo", label=".2e I- " %(M_i_prebio))
176 axes[2].plot(wv_febf4, absorbance_gelbstoff, "ko", \
177 label=".2e SDP" %(M_gelbstoff_prebio))

178 axes[2].plot(wv_febf4, absorbance_total, "ro", label="Total")

```

179

```
180 axes[2].set_xlabel("Wavelength (nm)") #titling x axis
181 axes[2].set_ylabel("Absorbance") #titling y axis
182 axes[2].set_title("Absorbance at %s cm" %(s))
183 axes[2].legend(loc="best", ncol=1,borderaxespad=0.5, fontsize=8) #creating legend
184 axes[2].set_yscale("log")
185 axes[2].set_xlim([195,320])
186
187 #graphing transmittance
188 axes[3].plot(wv_febf4, trans_br, "go", label=".2e Br-%(M_br_prebio))")
189 axes[3].plot(wv_febf4, trans_no3, "mo", label=".2e N03-%(M_no3_prebio))")
190 axes[3].plot(wv_febf4, trans_fe, "bo", label=".2e Fe2+" %(M_fe_prebio))
191 axes[3].plot(wv_febf4, trans_i, "yo", label=".2e I-%(M_i_prebio))")
192 axes[3].plot(wv_febf4, trans_gelbstoff, "ko", label=".2e SDP" %(M_gelbstoff_prebio))
193 axes[3].plot(wv_febf4, trans_total, "ro", label="Total")
194
195 axes[3].set_xlabel("Wavelength (nm)") #titling x axis
196 axes[3].set_ylabel("Transmittance") #titling y axis
197 axes[3].set_title("Transmittance at %s cm" %(s))
198 axes[3].legend(loc="best", ncol=1,borderaxespad=0.5, fontsize=8) #creating legend
199 #axes[2].set_yscale("log")
200 axes[3].set_xlim([195,320])
201
202 plt.subplots_adjust(left=0.125, bottom=0.1, right=0.9, top=0.9, wspace=0.01, \
203 hspace=0.4) #adjusting spacing
204 plt.savefig("Prebiotic_Ocean.pdf", orientation="portrait", papertype='letter', \
```

```
205 format="pdf") #saving graph as pdf  
206 plt.show() #display graph##
```

Appendix C Python Code for the Modelling of a Pre-biotic Lake

```
1      #!/usr/bin/env python3  
2 # -*- coding: utf-8 -*-  
3 """  
4 Created on Mon Jul 29 14:51:12 2019  
5  
6 @author: azrahaseki  
7 """  
8  
9 #importing useful libraries  
10 import matplotlib.pyplot as plt  
11 import numpy as np  
12 import pdb  
13  
14 s = 100 #setting depth in units cm  
15  
16 #specifiying concentrations of ions  
17 M_no3_lake = 0.000001 #1 uM  
18 M_so3_lake = 0.000050 #50 uM  
19 M_hso3_lake = 0.000050 #50 uM
```

```

20
21 #importing data
22 wv_quickenden, molabs_quickenden = np.genfromtxt('./Processed-Data/quickenden.dat', \
23 skip_header=2, unpack=True, usecols=(0,1)) #nm, M^-1
24 wv_no3, molabs_no3 = np.genfromtxt('./Processed-Data/mack_no3.dat', \
25 skip_header=2, unpack=True, usecols=(0,1)) #nm, M^-1 cm^-1
26 wv_so3, molabs_so3 = np.genfromtxt('./Processed-Data/hayon_so3.dat', \
27 skip_header=2, unpack=True, usecols=(0,1)) #nm, M^-1 cm^-1
28 wv_hso3, molabs_hso3 = np.genfromtxt('./Processed-Data/hayon_hso3.dat', \
29 skip_header=2, unpack=True, usecols=(0,1)) #nm, M^-1 cm^-1
30
31 #interpolating to Quickenden wavelength
32 molabs_no3_adjusted = np.interp(wv_quickenden, wv_no3, molabs_no3)
33 molabs_so3_adjusted = np.interp(wv_quickenden, wv_so3, molabs_so3)
34 molabs_hso3_adjusted = np.interp(wv_quickenden, wv_hso3, molabs_hso3)
35
36 #calculating total absorptivity
37 absorptivity_total = molabs_no3_adjusted * M_no3_lake \
38 + molabs_so3_adjusted * M_so3_lake + molabs_hso3_adjusted * M_hso3_lake
39 np.savetxt("./Processed-Data/constructed_lake.dat", \
40 np.column_stack((wv_quickenden, absorptivity_total)), delimiter=",", newline="\n", \
41 fmt="%3.1f %1.6e", header="Constructed molar absorbtivity of the modern \
42 ocean\nWavelength (nm), Absorptivities (cm^-1)")
43
44
45 #calculating absorbances

```

```

46 absorbance_no3 = molabs_no3_adjusted * M_no3_lake * s
47 absorbance_so3 = molabs_so3_adjusted * M_so3_lake * s
48 absorbance_hso3 = molabs_hso3_adjusted * M_hso3_lake * s
49 absorbance_total = absorbance_no3 + absorbance_so3 + absorbance_hso3

50

51 #calculating transmittances

52 trans_no3 = 10 ** (-1 * absorbance_no3)
53 trans_so3 = 10 ** (-1 * absorbance_so3)
54 trans_hso3 = 10 ** (-1 * absorbance_hso3)
55 trans_total = 10 ** (-1 * absorbance_total)

56 ##### graphing lake #####
57 fig, axes = plt.subplots(4,figsize=(6.5,12.))

58

59 #graphing molar absorptivities

60 axes[0].plot(wv_quickenden, molabs_no3_adjusted, "bo", label="NO$_3^-$")
61 axes[0].plot(wv_quickenden, molabs_so3_adjusted, "go", label="SO$_4^{2-}$")
62 axes[0].plot(wv_quickenden, molabs_hso3_adjusted, "yo", label="HSO$_3^-")
```

63

```

64 axes[0].set_xlabel("Wavelength (nm)") #titling x axis
65 axes[0].set_ylabel("Molar Absorptivity (M$^{-1}$ cm$^{-1}$)") #titling y axis
66 axes[0].set_title("Molar Absorptivities")
67 axes[0].legend(loc="best", ncol=2,borderaxespad=0.4, fontsize=10) #creating legend
68 axes[0].set_yscale("log")
69 #axes[0].set_xlim([195,320])
```

70

```

71 #graphing absorptivities
```

```

72 axes[1].plot(wv_quickenden, molabs_no3_adjusted * M_no3_lake, "bo", \
73 label=".2e NO$_3^-$ % (M_no3_lake))

74 axes[1].plot(wv_quickenden, molabs_so3_adjusted * M_so3_lake, "go", \
75 label=".2e SO$_3^{2-}$ % (M_so3_lake)")

76 axes[1].plot(wv_quickenden, molabs_hso3_adjusted * M_hso3_lake, "yo", \
77 label=".2e HSO$_3^-$ % (M_hso3_lake))

78 axes[1].plot(wv_quickenden, absorptivity_total, "ro", label="Total absorbtivity")

79

80 axes[1].set_xlabel("Wavelength (nm)") #titling x axis

81 axes[1].set_ylabel("Absorptivities (cm^-1)") #titling y axis

82 axes[1].set_title("Absorbtivities")

83 axes[1].legend(loc="best", ncol=2, borderaxespad=0.4, fontsize=10) #creating legend

84 axes[1].set_yscale("log")

85

86 #graphing absorbance

87 axes[2].plot(wv_quickenden, absorbance_no3, "bo", label=".2e NO$_3^-$ % (M_no3_lake))

88 axes[2].plot(wv_quickenden, absorbance_so3, "go", label=".2e SO$_3^{2-}$ % (M_so3_lake))

89 axes[2].plot(wv_quickenden, absorbance_hso3, "yo", \
90 label=".2e HSO$_3^-$ % (M_hso3_lake))

91 axes[2].plot(wv_quickenden, absorbance_total, "ro", label="Total")

92

93 axes[2].set_xlabel("Wavelength (nm)") #titling x axis

94 axes[2].set_ylabel("Absorbance") #titling y axis

95 axes[2].set_title("Absorbance at %s cm" %(s))

96 axes[2].legend(loc="best", ncol=2, borderaxespad=0.4, fontsize=8) #creating legend

97 axes[2].set_yscale("log")

```

```

98 #axes[2].set_xlim([195,320])

99

100

101 #graphing transmittance

102 axes[3].plot(wv_quickenden, trans_no3, "bo", label=".2e NO$_3^-$ %(M_no3_lake))
103 axes[3].plot(wv_quickenden, trans_so3, "go", label=".2e SO$_3^{2-}$ %(M_so3_lake))
104 axes[3].plot(wv_quickenden, trans_hso3, "yo", label=".2e HSO$_3^-$ %(M_hso3_lake))
105 axes[3].plot(wv_quickenden, trans_total, "ro", label="Total")

106

107 axes[3].set_xlabel("Wavelength (nm)") #titling x axis
108 axes[3].set_ylabel("Transmittance") #titling y axis
109 axes[3].set_title("Transmittance at %s cm" %(s))
110 axes[3].legend(loc="best", ncol=1,borderaxespad=0.4, fontsize=8) #creating legend
111 #axes[2].set_yscale("log")
112 #axes[3].set_xlim([195,320])

113

114 leg = plt.legend()
115 leg.get_frame().set_edgecolor('k')
116
117 plt.subplots_adjust(left=0.125, bottom=0.1, right=0.9, top=0.9, wspace=0.01, \
118 hspace=0.4) #adjusting spacing
119 #plt.savefig("Lake.pdf", orientation="portrait", papertype='letter', format="pdf") \
120 #saving graph as pdf
121 plt.show() #display graph##

```
